*Journal of Bioenergetics and Biomembranes, Vol. 25, No. 3, 1993*

*Minireview*

# What Information Do Inhibitors Provide about the Structure of the Hydroquinone Oxidation Site of Ubihydroquinone: Cytochrome *c* Oxidoreductase?

**T. A. Link,[1] U. Haase,[1] U. Brandt,[1] and G. von Jagow[1]**

*Received November 5, 1992; accepted January 2, 1993*

The Q cycle mechanism of the $bc_1$ complex requires two quinone reaction centers, the hydroquinone oxidation ($Q_P$) and the quinone reduction ($Q_N$) center. These sites can be distinguished by the specific binding of inhibitors to either of them. A substantial body of information about the hydroquinone oxidation site has been provided by the analysis of the binding of $Q_P$ site inhibitors to the $bc_1$ complex in different redox states and to preparations depleted of lipid or protein components as well as by functional studies with mutant $bc_1$ complexes selected for resistance toward the inhibitors. The reaction site is formed by at least five protein segments of cytochrome *b* and parts of the iron–sulfur protein. At least two different binding sites for $Q_P$ site inhibitors could be detected, one for the methoxyacrylate-type inhibitors binding predominantly to cytochrome *b*, the other for the chromone-type inhibitors and hydroxyquinones binding predominantly to the iron–sulfur protein. The interactions with the protein segments, between different protein segments, and between protein and ligands (substrate, inhibitors) are discussed in detail and a working model of the $Q_P$ pocket is proposed.

KEY WORDS: $bc_1$ complex; cytochrome *b*; iron–sulfur protein; $Q_P$ pocket; model; MOA inhibitor; myxothiazol; stigmatellin; binding analysis; mutant analysis.

## INTRODUCTION: Q-CYCLE

The Q-cycle[2] scheme proposed by P. Mitchell in 1976 is now widely accepted as the scheme of electron and proton transfer through ubihydroquinone: cytochrome *c* oxidoreductase (Mitchell, 1976; von Jagow *et al.*, 1986; Trumpower, 1990). The most simple version is shown in Fig. 1; however, some refinements may be required to account for all experimental observations.

The essential features of the Q-cycle are: (i) the existence of two pathways for electrons, a high-potential pathway at the P-side of the membrane via the iron–sulfur cluster and cytochrome $c_1$ to the electron acceptor cytochrome *c*, and a transmembrane low-potential pathway consisting of both hemes *b*; (ii) recycling of half of the electrons back into the quinone pool; and (iii) a vectorial arrangement of the proton release and uptake pathways.

On oxidation of ubihydroquinone, two protons are released to the P-side and the first electron is transferred onto the iron–sulfur cluster while the second electron goes to heme $b_L$ and from there across the membrane to heme $b_H$. Heme $b_H$ reduces a molecule of ubiquinone to ubisemiquinone which is stabilized by interaction with the protein environment. In order to complete the cycle, a second molecule of ubihydroquinone is oxidized with release of two protons to the P-side, the first electron again being transferred onto the iron–sulfur cluster and the second electron via heme $b_L$ to heme $b_H$ where it reduces ubisemiquinone to ubihydroquinone with the uptake

[1] Universitätsklinikum Frankfurt, ZBC, D-6000 Frankfurt/Main 70, Germany.

[2] Abbreviations: MOA, *E*-β-methoxyacrylate; MOA-stilbene, (*E*)-methyl-3-methoxy-2-(4′-*trans*-stilbenyl)acrylate; Q, quinone; $QH_2$, hydroquinone; UHDBT, 5-undecyl-6-hydroxy-4,7-dioxobenzothiazol, UHNQ, 3-undecyl-2-hydroxynapthoquinone.



0145-479X/93/0600-0221$07.00/0 

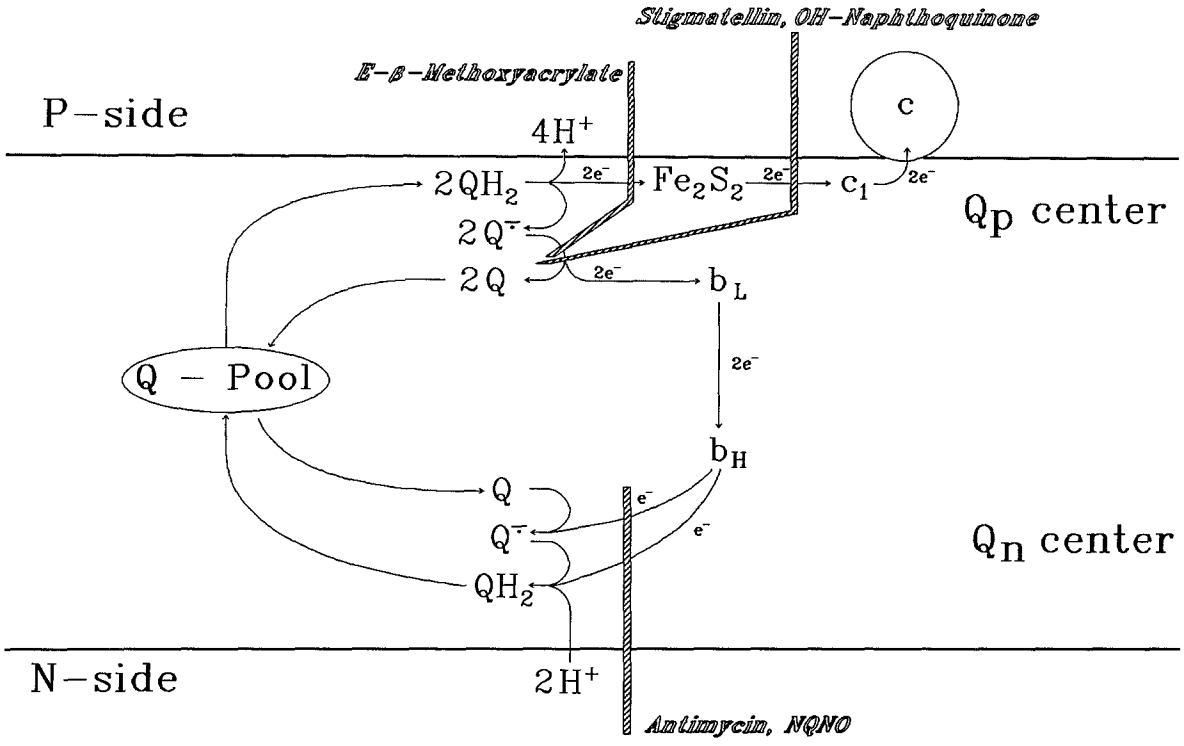


**Fig. 1.** Q cycle scheme of the $bc_1$ complex (cf. text). The points of inhibition of various inhibitors are indicated.

of two protons from the N-side. During one complete cycle, two ubihydroquinone molecules are oxidized and one ubiquinone is re-reduced to ubihydroquinone; the net reaction therefore is the oxidation of one ubihydroquinone, reduction of two molecules of cytochrome *c*, uptake of two protons from the N-side, and release of four protons to the P-side. The stoichiometry of the complex is 4 $H^+$ released on the outside and 2 charges transported across the membrane per $2e^-$ transferred to cytochrome $c_1$.

$$QH_2 + 2\ \text{cyt}\ c^{ox} + 2H_N^+ \rightarrow Q + 2\,\text{cyt}\ c^{red} + 4H_p^+$$

## CLASSIFICATION OF THE INHIBITORS

The Q cycle mechanism described above requires the existence of two quinone reaction sites. These can be distinguished by the binding of specific inhibitors. Three types of inhibitors block the $Q_N$ (quinone reduction) center: antimycin, funiculosin, and hydroxyquinoline-N-oxides. Electron transfer through the $Q_P$ site can be blocked by a multitude of compounds (von Jagow and Link, 1986; von Jagow and Brandt, 1991) (Fig. 2):

1. 2-Hydroxy-1,4-benzoquinone derivatives. These inhibitors resemble the substrate ubiquinone but contain an additional 2-hydroxy group. The oxidized hydroxyquinones bind to the reduced iron–sulfur protein and shift its midpoint potential ($E_{m,7}$) toward more positive values (Trumpower and Haggerty, 1980; Bowyer *et al.*, 1982; Matsuura *et al.*, 1983).

2. Stigmatellins, i.e., chromone derivatives. These components also bind to the reduced iron–sulfur protein and shift its midpoint potential. In addition, they also bind to cytochrome *b*, inducing a spectral change mostly of heme $b_L$ (Thierbach *et al.*, 1984; von Jagow and Ohnishi, 1985; Ohnishi *et al.*, 1988).

3. MOA inhibitors. These inhibitors all contain the *E*-β-methoxyacrylate group, which resembles part of the ubiquinone structure. The inhibitors have an aromatic side chain attached in the α-position (MOA-stilbene, strobilurin, oudemansin) or in the β-position (myxothiazol). They bind to cytochrome *b*, inducing a red shift of the α- and γ-bands of heme $b_L$ (Becker *et al.*, 1981; Thierbach and Reichenbach, 1981; von Jagow and Engel, 1981; Brandt *et al.*, 1988). CPMB-oxime, an aromatic ketoxime, shows similar behavior although it does not contain the acrylate function (Brandt and von Jagow, 1991a).

4. Zinc ions. $Zn^{2+}$ ions bind specifically to the $Q_P$

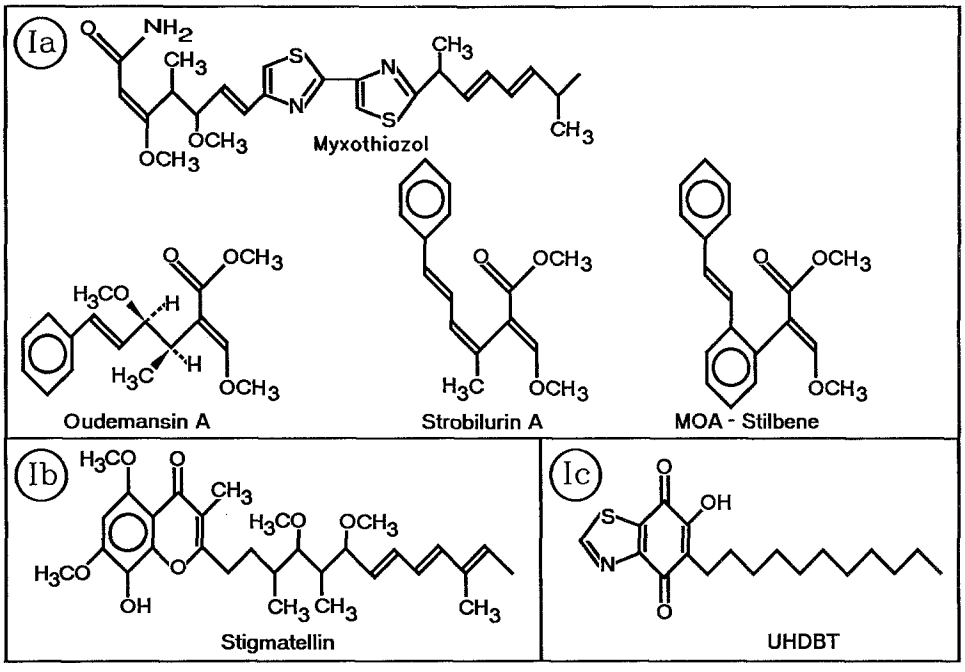


Fig. 2. Structures of selected $Q_p$ inhibitors. Upper box: methoxyacrylate inhibitors. UHDBT is a representative of the hydroxyquinone inhibitors.

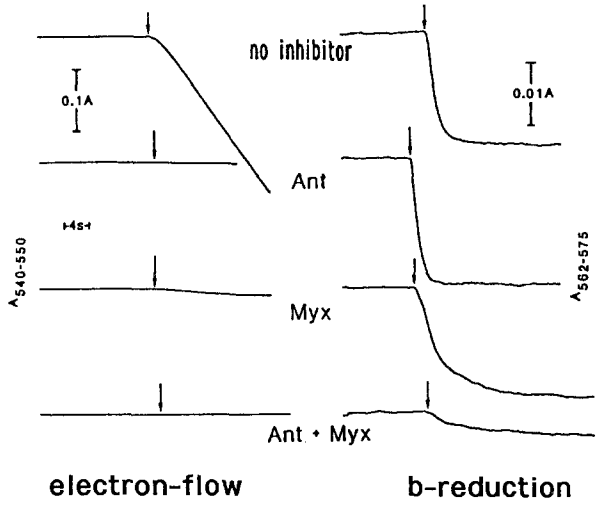


Fig. 3. Inhibition of bovine heart $bc_1$ complex by $Q_P$ and $Q_N$ inhibitors. The start of the reaction by addition of substrate is indicated by the arrow. Antimycin is a representative of a $Q_N$ inhibitor, myxothiazol a representative of a $Q_P$ inhibitor. Addition of either a $Q_P$ or a $Q_N$ inhibitor inhibits catalytic electron transfer from ubihydroquinone to cytochrome *c* monitored at 540–550 nm (left row). Reduction of cytochrome *b* by hydroquinone monitored at 575–562 nm (right row) is only inhibited if both inhibitors are added simultaneously ("double kill").

center of bovine cytochrome *c* reductase (Lorusso *et al.*, 1991; Link *et al.*, submitted for publication).

The two quinone reaction sites function independently, i.e., cytochrome *b* can be reduced through either the $Q_P$ site (forward reaction) or through the $Q_N$ site (reverse reaction). Therefore, cytochrome *b* can still be reduced by hydroquinone if either a $Q_P$ or $Q_N$ site inhibitor is added although steady-state electron transfer through the $bc_1$ complex is blocked (Fig. 3). Only simultaneous addition of $Q_P$ *and* $Q_N$ site inhibitors leads to an inhibition of *b* reduction (double kill, Fig. 3) (von Jagow and Engel, 1981). The separation of the $Q_P$ and $Q_N$ reaction sites is also indicated by the fact that the inhibitors have large effects on the spectra of the heme which is close to the respective binding site and only minor spectral effects on the distant heme (Rich *et al.*, 1990).

## METHODS FOR STUDYING INHIBITOR BINDING

A preliminary characterization of $bc_1$ complex inhibitors could be obtained by the determination of the apparent $I_{50}$ values, i.e., the concentration for half-inhibition of steady-state electron flow. Two methods could be used for this purpose: titration of

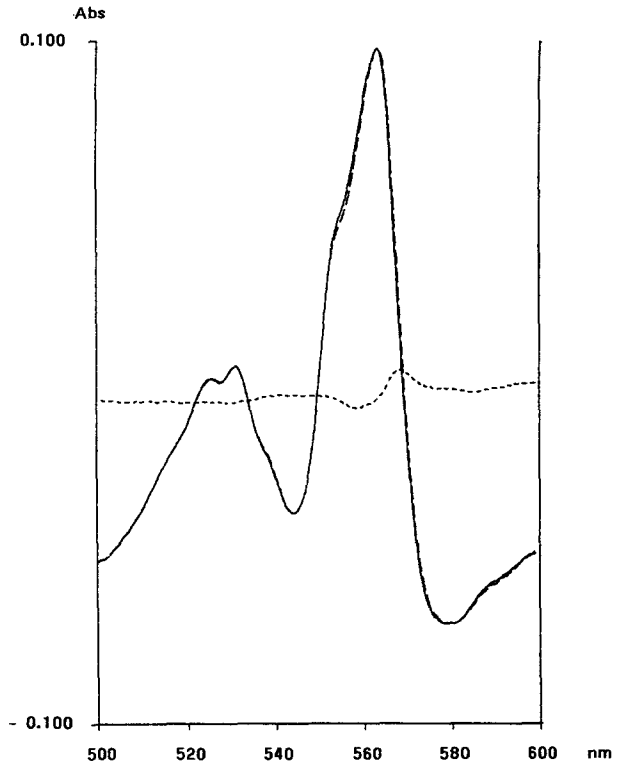


**Fig. 4.** Red shift of cytochrome *b* induced by MOA-stilbene. $bc_1$ complex (6$\mu$M cytochrome *b*) was first reduced by dithionite and measured against a ferricyanide-oxidized sample (solid line). Then a tenfold excess of MOA-stilbene was added to the sample cuvette and the spectrum was recorded again (dashed line). The dotted line shows the red shift spectrum which is the difference between the spectra obtained with and without addition of inhibitor in the presence of dithionite.

the inhibition of mitochondrial cytochrome *c* reductase activity and titration of the inhibition of mitochondrial electron transfer from succinate to oxygen (Brandt *et al.*, 1988). The advantage of the latter method is the rapid way in which data are obtained.

Single turnover reduction kinetics allow the determination of the site of inhibition. Reduction of cytochrome $c_1$ is only blocked by $Q_P$ site inhibitors, whereas $Q_N$ site inhibitors do not inhibit this reaction. The reduction of cytochrome *b* could only be blocked if both type of inhibitors were added together. This type of experiment describes the so-called "double kill" phenomenon.

Some of the inhibitors induce a spectral shift of the *b* hemes. The $Q_N$ inhibitor antimycin A induces a stable and symmetrical bathochromic shift of both the $\alpha$- and $\gamma$-bands of reduced heme $b_H$. The $Q_P$-site inhibitors of the chromone and methoxyacrylate type shift mainly the spectrum of reduced heme $b_L$ (von Jagow and Engel, 1981; Rich *et al.*, 1990). These red shifts are proportional to the amount of bound inhibitor. The peak-to-peak amplitude of the $\alpha$-shift induced by MOA-stilbene is about 7–8% of the magnitude of the absorption signal (Fig. 4). The dissociation constants of the inhibitors can be determined by titrating the reduced enzyme in a dual-wavelength mode. Using a standard binding equation, Brandt *et al.* (1988) calculated the values for bound and free inhibitor by means of a computer fit of the titration curve. The dissociation constant of the inhibitors determined by this method reflects the binding to the reduced form of the enzyme.

The fluorescence of several fluorescent inhibitors is quenched upon binding to the $bc_1$ complex. Fluorescence quench titration monitors the inhibitor rather than the enzyme; therefore, this technique is suited to study different redox states of the enzyme, whereas the red-shift titration is limited to the reduced enzyme. Binding of inhibitors to the oxidized enzyme, ascorbate-reduced enzyme (only the high potential chain, i.e., iron–sulfur cluster and heme $c_1$ reduced), hydroquinone-reduced enzyme (high potential chain and heme $b_H$ reduced), and dithionite, i.e., fully reduced enzyme, can be compared under identical experimental conditions (Brandt and von Jagow, 1991a).

Fluorescent inhibitors of the $bc_1$ complex are the $Q_N$ site inhibitors antimycin A and NQNQ (Berden and Slater, 1970, 1972; van Ark and Beaden, 1977) and the $Q_P$ site inhibitor MOA-stilbene (Brandt and von Jagow, 1991b). The $K_D$ for nonfluorescent inhibitors could be determined indirectly by analyzing their competition with fluorescent inhibitors. While the red-shift titration requires isolated $bc_1$ complex, fluorescence quench titration can also be performed on mitochondrial membrane preparations.

Binding of hydroxyquinones and stigmatellin to the $bc_1$ complex can be monitored specifically by EPR spectroscopy of the reduced iron–sulfur cluster. The iron–sulfur cluster with bound stigmatellin shows a specific $g_x$ signal at $g = 1.79$ which differs from the spectrum without inhibitor or with myxothiazol bound (von Jagow *et al.*, 1984; Ohnishi *et al.*, 1988).

## INHIBITOR-RESISTANT MUTANTS

Inhibitor-resistant mutants have been character-

ized in mouse (Howell, 1990), yeast (Tron *et al.*, 1991; Geier *et al.*, 1992) and *Rhodobacter capsulatus* (Robertson *et al.*, 1990). The mutants were selected for respiratory (mouse: Howell and Gilbert, 1988); yeast: di Rago *et al.*, 1989) or photosynthetic (*Rhodobacter*: Daldal *et al.*, 1989) growth in the presence of either $Q_P$ or $Q_N$ site inhibitors. The detailed analysis of inhibitor binding and enzyme kinetic parameters of the mutants carrying single point mutations in cytochrome *b* has provided information about individual amino acid residues involved in the reaction pockets.

## BINDING OF INHIBITORS TO DIFFERENT PARTS OF THE $Q_P$ POCKET: BIOCHEMICAL STUDIES

Hydroxyquinones bind predominantly to the iron–sulfur protein while MOA inhibitors bind mainly to cytochrome *b* . Stigmatellin is the only inhibitor known so far which affects both proteins forming the $Q_P$ pocket. Although $Q_P$ site inhibitors bind to different parts of the pocket, they bind competitively to each other, i.e., tighter binding inhibitors displace weaker binding inhibitors from their binding site (von Jagow *et al.*, 1984; von Jagow and Ohnishi, 1985; Brandt and von Jagow, 1991b).

Upon removal of the iron–sulfur protein from the $bc_1$ complex, the $K_D$ for stigmatellin increases from below 1 nM to >10 $\mu$M; the residual affinity of the iron–sulfur depleted complex for stigmatellin as determined through competitive analysis of MOA binding is similar to the affinity for the weaker inhibitor UHNQ (Brandt *et al.*, 1991). It is therefore not clear whether this low-affinity binding reflects the specific interactions between cytochrome *b* and stigmatellin or UHNQ, two inhibitors binding predominantly to the iron–sulfur protein, or whether the $K_D$ indicative of more unspecific competition of the two inhibitors for a MOA-stilbene binding site (Brandt and von Jagow, 1991b).

A red shift of cytochrome *b* of the iron–sulfur depleted complex was observed upon binding of oudemansin A, a MOA type inhibitor, and the $K_D$ was almost unchanged if the effect of the delipidation was accounted for (Brandt *et al.*, 1991).

Zinc ions bind to $bc_1$ complex depleted of the iron–sulfur protein with an affinity which is two- to threefold higher than that of complete $bc_1$ complex (Link *et al.*, submitted for publication). Binding of $Zn^{2+}$ was not affected by binding of a MOA inhibitor. Therefore, $Zn^{2+}$ ions seem to bind to different residues of cytochrome *b* than the other inhibitors.

## BINDING OF INHIBITORS TO DIFFERENT PARTS OF THE $Q_P$ POCKET: MUTANT STUDIES

By analyzing the binding of $Q_P$ inhibitors to mutants selected for inhibitor resistance, ten amino acid positions of cytochrome *b* could be identified where mutations changed the binding constants of at least one of the inhibitors. These ten positions are spread over five topologically different regions of the protein at or near the P-side of the membrane (the sequence numbering follows the sequence of yeast cytochrome *b*) (Fig.5, Table I):

- —Helix III: Ile-125 (Met in *Rhodobacter* where the mutant was obtained) and Phe-129.
- —Loop between helix III and surface helix IV: Gly-137 and Gly-143
- —Surface helix IV: Ile-147 and Thr-148
- —Loop between helices VI and VII: Asn-256 and Leu-275
- —Helix VII: Val-292 and Met-295 (Leu in mouse where the mutant was obtained)

The residues in helix structures are either adjacent (helix IV) or one turn of the helix apart on the same side of the transmembrane helices III (= helix C) and VII (= helix F). The fact that in each helix at least two positions were identified gives additional strength to the view that the quadrants of the helices where the respective positions are located are involved in the formation of the walls of the $Q_P$ pocket.

For this discussion we have looked at all mutations available neglecting possible species differences. Although the results are generally consistent, some differences are found, e.g., between the electron transfer capability of the Phe-129 → Leu mutation in yeast and in *Rhodobacter*: the yeast mutant has more than 50% of the wild type activity, while the *Rhodobacter* strain has only about 10% residual activity (Robertson *et al.*, 1990: Tron *et al.*, 1991). Yeast cytochrome *b* has isoleucine in position 125; mutation of methionine in the homologous position 144 in *Rhodobacter* to isoleucine confers resistance to myxothiazol and stigmatellin.

The mutations induce a change of the dissociation constant $K_D$ of the inhibitors. Although the

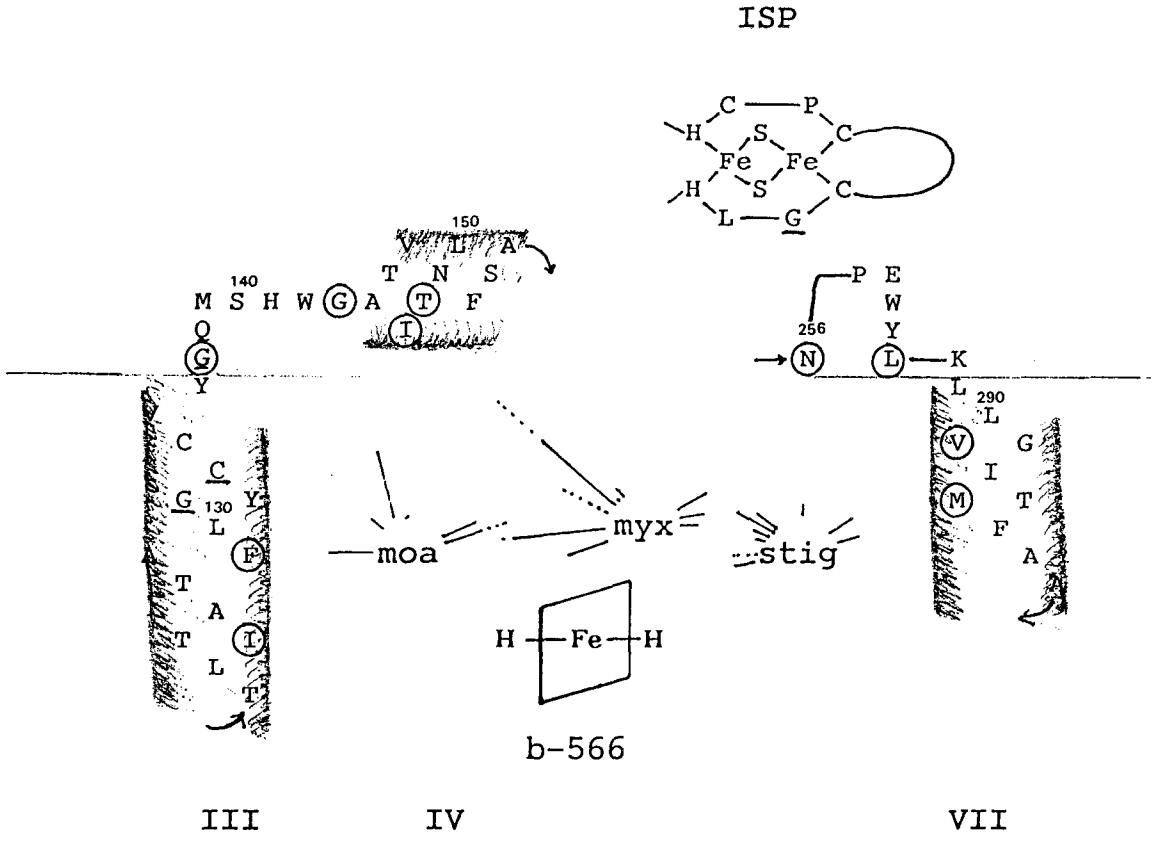


**Fig. 5.** Structure of the $Q_P$ pocket close to heme $b_L$ (heme *b*-566). Helix III, the loop between helices III and IV, helix IV, the loop between helices VI and VII, helix VII, and the iron sulfur protein are involved in the formation of the pocket. Residues where mutations give rise to functional deficiency have been underlined. Residues where mutations alter inhibitor binding have been encircled. The length of the lines pointing from the three inhibitors toward these residues indicate the $\Delta\Delta G$ values observed for the respective inhibitors (see Table I). The three inhibitors do not bind simultaneously but displace each other from the binding site. The figure shows an exploded view of the pocket which must be thought to be folded into a compact structure in three dimensions.

energy of binding of the inhibitors cannot be determined since the measured values of $K_D$ are apparent values which include a large contribution from the phase distribution of the hydrophobic inhibitors, the *difference* in the energy of binding to the wild type and to the mutant complex can be calculated from the resistance $R = K_D(\text{mutant})/K_D(\text{wild type})$:

$$\Delta\Delta G_{\text{binding}} = R \cdot T \cdot \ln(R)$$
$$= 5.7 \cdot \log(R)\,\text{kJ/mole}$$

Binding of different classes of inhibitors is impaired to a different extent in the mutants studied. Unfortunately, a complete picture cannot be obtained since the change of the affinity has not been determined for all inhibitors in all of the mutants. Nevertheless, the following can be deduced from mutants studied so far (Fig. 5):

—Binding of myxothiazol is mostly affected by mutations in positions 143 (24 kJ/mole) and 129 (16–17 kJ/mole).

—Binding of other MOA inhibitors is affected to a lesser extent $\leq$ 10 kJ/mole.

—Binding of stigmatellin is altered mostly by mutations in helices III and IV; the difference in binding energy is $\leq$ 10 kJ/mole. This is consistent with the observation that stigmatellin binds predominantly to the iron–sulfur protein, as follows from the large $K_D$ shift upon removal of the iron–sulfur protein. For the hydroxyquinone inhibitor, UHDBT, a loss in binding energy of 2–3 kJ/mole is observed in those *Rhodobacter* mutants where binding of stigmatellin is impaired. The notable exception is mutant Phe-129 → Leu (position 144 in *Rhodobacter*) where binding of UHDBT is

**Table I.** Alterations in Binding Energies of Inhibitors to the $bc_1$ Complex Caused by Point Mutations in Cytochrome $b$[a]

| Position | | Amino acid substitution | Species | ΔΔG (binding), kJ/mol | | | | Activity | Reference |
|---|---|---|---|---|---|---|---|---|---|
| Yeast | Rb | | | Myxothiazol | MOA | Stigmatellin | UHDBT | | |
| 125 | 140 | M → I | r | 7 | | 5 | 2 | 100% | Robertson *et al.*, 1990 |
| 129 | 144 | F → S | r | 16 | | 0 | 0 | <100% | Robertson *et al.*, 1990 |
| 129 | 144 | F → L | r | 16 | 0 | 4 | 6 | 10% | Robertson *et al.*, 1990 |
| 129 | | F → L | y | 17 | 7 | −1 | | <100% | Tron *et al.*, 1991 |
| 137 | 152 | G → S | r | 9 | | 2 | 0 | <100% | Robertson *et al.*, 1990 |
| 137 | | G → R | y | 5 | 2 | <2 | | >100% | Geier *et al.*, 1992 |
| 137 | | G → E | y | 5 | | | | 46% | Tron and Lemesle-Meunier, 1990 |
| 137 | | G → V | y | 2 | | | | 60% | Tron and Lemesle-Meunier, 1990 |
| 143 | | G → A | m | 24 | >0 | 3 | | | Howell, 1990 |
| 147 | | I → F | y | 0 | 0 | 7 | | ≈50% | Tron *et al.*, 1991 |
| 148 | 163 | T → A | r | 3 | | >4 | 3 | 100% | Robertson *et al.*, 1990 |
| 148 | | T → M | m | −2 | | >4 | | | Howell, 1990 |
| 256 | | N → Y | y | (27[b]) | 6 | <2 | | 25% | Geier *et al.* 1992 |
| 275 | | L → S | y | >0 | >0 | | | | Gießler, unpublished |
| 292 | 333 | V → A | r | 4 | | >5 | 2 | 100% | Robertson *et al.*, 1990 |
| 295 | | L → F | m | 3 | | 4 | | | Howell, 1990 |

[a] Species: m, mouse; r, Rhodobacter (Rb); y, yeast. $\Delta\Delta G$ denotes the difference in binding energy $\Delta G$ between the mutant and the wild type enzymes. Positive values denote a loss of binding energy of the inhibitor in the mutants.

[b] In isolated $bc_1$ which has lost the iron–sulfur protein.

weakened by 6 kJ/mole. This mutant has only about 10% residual activity.

## REDOX DEPENDENCE OF INHIBITOR BINDING TO THE $Q_P$ POCKET

The binding of hydroxyquinones and stigmatellin depends on the redox state of the iron–sulfur cluster. Upon its oxidation, binding of the hydroxyquinones UHNQ and UHDBT is weakened by 7–10 kJ/mole (Matsuura *et al.*, 1983; von Jagow *et al.*, 1984) and binding of stigmatellin is weakened by 24 kJ/mole (von Jagow and Ohnishi, 1985). Binding of MOA inhibitors to cytochrome *b* is stronger by 2 kJ/mole if the iron–sulfur cluster is oxidized (Brandt *et al.*, 1991). The binding of $Q_P$ site inhibitors is very little affected by the redox state of heme $b_L$ (Rich *et al.*, 1990). After removal of the iron–sulfur protein from the $bc_1$ complex, MOA-stilbene binds 2 kJ/mole tighter to reduce cytochrome *b* than to the oxidized cytochrome *b* while no change was observed in the presence of the iron–sulfur protein (Brandt *et al.*, 1991). The redox-dependent changes of the binding affinity of $Q_P$ site inhibitors were interpreted in terms of a "catalytic switch" occurring during turnover at the $Q_P$ site (Brandt and von Jagow, 1991b).

## BINDING OF QUINONES TO THE $Q_P$ POCKET

Binding of quinones and hydroquinones to the reduced iron–sulfur cluster can be monitored through specific changes of the $g_x$ signal of the cluster (Robertson *et al.*, 1990). The iron–sulfur cluster without quinone has a broad $g_x$ signal around $g = 1.765$; when oxidized quinone is bound, the $g_x$ signal appears at $g = 1.78$; when reduced hydroquinone is bound, the signal becomes sharper at $g = 1.80$. Ding *et al.*, (1992) have reported that two quinone molecules can be bound simultaneously in the $Q_P$ pocket of the $bc_1$ complex of *Rhodobacter capsulatus*. Binding of either stigmatellin or myxothiazol abolished binding of both quinone and hydroquinone. Addition of myxothiazol to isolated bovine heart $bc_1$ complex displaced the quinone UHDBT (von Jagow *et al.*, 1984) and changed the $g_x$ signal to the form which coincides with displacement of ubiquinone (Trumpower, 1981) and which is observed in the isolated iron–sulfur protein devoid of quinone (Ding *et al.*, 1992).

On the other hand, hydroquinone behaved noncompetitively in kinetic assays and was not able to displace weakly binding MOA inhibitors from their binding site on cytochrome *b* (Brandt *et al.*, 1988). This apparent noncompetitive inhibition was considered indicative of conformational changes of the $Q_P$ site induced by binding of inhibitors.

There is an apparent contradiction between experiments showing that inhibitors displace quinones but that quinones cannot displace the inhibitors. One possible explanation that one might conceive is that quinones do not bind directly at the reaction site but first to primary binding sites at the interface between protein and lipid so that the excess of quinone molecules does not directly compete with molecules in the reaction site. These binding sites would not be detected in a kinetic analysis. This idea is speculative but could also explain why the isolated complex looses its activity completely on delipidation although redox centers and binding of MOA inhibitors seem to be almost unchanged (Schägger *et al.*, 1990).

The recognition of the quinone headgroup by the quinone binding site has been tested by comparing the activity of quinone derivatives (Gu *et al.*, 1990). Recently, it has been shown that binding of phenolic derivatives to the $Q_P$ pocket depends on the structure and conformation of the alkyl side chain (Saitoh *et al.*, 1992). The pocket requires a side chain conformation perpendicular to the quinone ring plane in contrast to the $Q_B$ site of the photoreaction center. The restriction of a bond rotation upon binding adversely affects binding by 5–6 kJ/mole (Page and Jencks, 1971); therefore binding of derivatives with restricted rotation is favorable by this extent.

## INTERACTIONS BETWEEN PROTEIN AND LIGANDS IN THE $Q_P$ POCKET

The loss of binding energy of the inhibitors observed for the mutations obtained so far is in the range between 2 and 24 kJ/mole. These energy differences are low compared to standard interaction energies. H bonds have a bond energy of at least 12–21 kJ/mole; the energy contribution of a single van der Waals interaction between two hydrogenated carbon atoms has been estimated as 0.8 kJ/mole (Schulz and Schirmer, 1979). In view of these numbers, most of the resistant mutations having a loss of binding energy of less than 10 kJ/mole would involve the loss of only a few van der Waals interactions.

Only a few changes in the $Q_P$ pocket have an effect on the binding energy of an inhibitor of more than 10 kJ/mole: reduction of the iron–sulfur cluster on binding of stigmatellin and mutations in positions 129 and 143 on binding of myxothiazol. Reduction of the iron–sulfur protein at neutral pH leads to a change from partial to full protonation of a residue with a redox-dependent p$K$ value (Prince and Dutton, 1976; Link *et al.*, 1992); this might induce an additional H bond between the iron–sulfur protein and stigmatellin in addition to electrostatic effects.

The strongly resistant mutants do not involve hydrogen-bonding residues. This indicates that a major change of the hydrogen-bonding pattern in the $Q_P$ pocket will not only prevent inhibitor binding but also quinone binding, thus leading to deficient rather than resistant mutants.

The resistant mutation in position 143 involves a substitution of the smallest amino acid glycine by alanine. Two possible explanations have to be considered for the large effect on binding energy: Steric interference of the additional methyl group with myxothiazol within the pocket or change of the conformation or flexibility of the peptide chain. Glycine differs from all other amino acids as it has a larger conformational freedom and is found frequently at the end of helices where the peptide chain turns. The mutation Gly → Asp in this position is incompatible with electron transfer activity (Robertson *et al.*, 1990).

In position 129, two distinct mutations were found which induce the same decrease of binding energy although the amino acid substitutions are quite different. The binding of myxothiazol of the mutants having serine and leucine in this position is identical while the mutants differ in their stigmatellin and hydroxyquinone binding. The effect of the mutation Phe-129 → Leu appears to be different in yeast and in *Rhodobacter* since the yeast mutant carrying this mutation has almost wild type activity while the activity of the *Rhodobacter* mutant is largely diminished. As both phenylalanine and leucine are hydrophobic residues, this indicates either a distortion of the structure of cytochrome *b* or specific aromatic interactions between the phenylalanine and the aromatic parts of quinone or inhibitor. The mutations have the same effect on myxothiazol binding as has the mutation Phe-216 → Ser in the L-subunit of the photoreaction center of *Rhodopseudomonas viridis* on *o*-phenanthroline binding (Sinning *et al.*, 1989). Residue 216 of the L-subunit interacts directly with quinone in the $Q_B$ site.

## INTERACTION BETWEEN PROTEIN DOMAINS OF THE $Q_P$ POCKET

The $Q_P$ pocket is formed by protein domains of both cytochrome *b* and the iron–sulfur protein. This was demonstrated unambiguously by the binding of stigmatellin to both proteins. Therefore, the two proteins must be in close contact near the stigmatellin binding site.

When the $bc_1$ complex of an inhibitor-resistant yeast mutant carrying the Asn-256 → Tyr mutation was isolated, it was found that the complex lost the iron–sulfur protein during the preparation procedure (Geier *et al.*, 1992). This was not due to unspecific denaturation of cytochrome *b* as the spectrum of cytochrome *b* was normal and as MOA inhibitors still bound to cytochrome *b*. Therefore, position 256 seems to be essential for interaction between cytochrome *b* and the iron–sulfur protein as well as for inhibitor binding. The binding of myxothiazol was decreased by at least 20 kJ/mole in the isolated complex with the iron–sulfur protein; this is in contrast to observations in the bovine heart enzyme where removal of the iron–sulfur protein does not alter the binding of MOA inhibitors. In the wild type yeast complex, the iron–sulfur protein cannot be removed except under partially denaturing conditions. Binding of the iron–sulfur protein to the rest of the $bc_1$ complex seems to occur both through hydrophobic domains near the N-terminus of the protein (González-Halphen *et al.*, 1991) and through contact with the protein domain carrying the redox cluster.

In both positions 137 and 256, inhibitor-resistant mutations were found (see above). In addition, some mutations in position 137 of cytochrome *b* induce respiratory deficiency. By analysis of revertants of a cytochrome *b*-deficient yeast mutant in position 137 (Gly → Glu), di Rago *et al.*, (1990a,b) identified a compensatory mutation in position 256 (Asn → Lys). This establishes a spatial relationship between these two residues and the iron–sulfur protein. The protein conformation at this site seems to be critical for function of the $Q_P$ pocket, and mutations in positions 137 and 256 will disturb the structure of the site.

## THE STRUCTURE OF THE $Q_P$ POCKET

The following structure of cytochrome *b* and the $Q_P$ pocket emerges from structure prediction, model

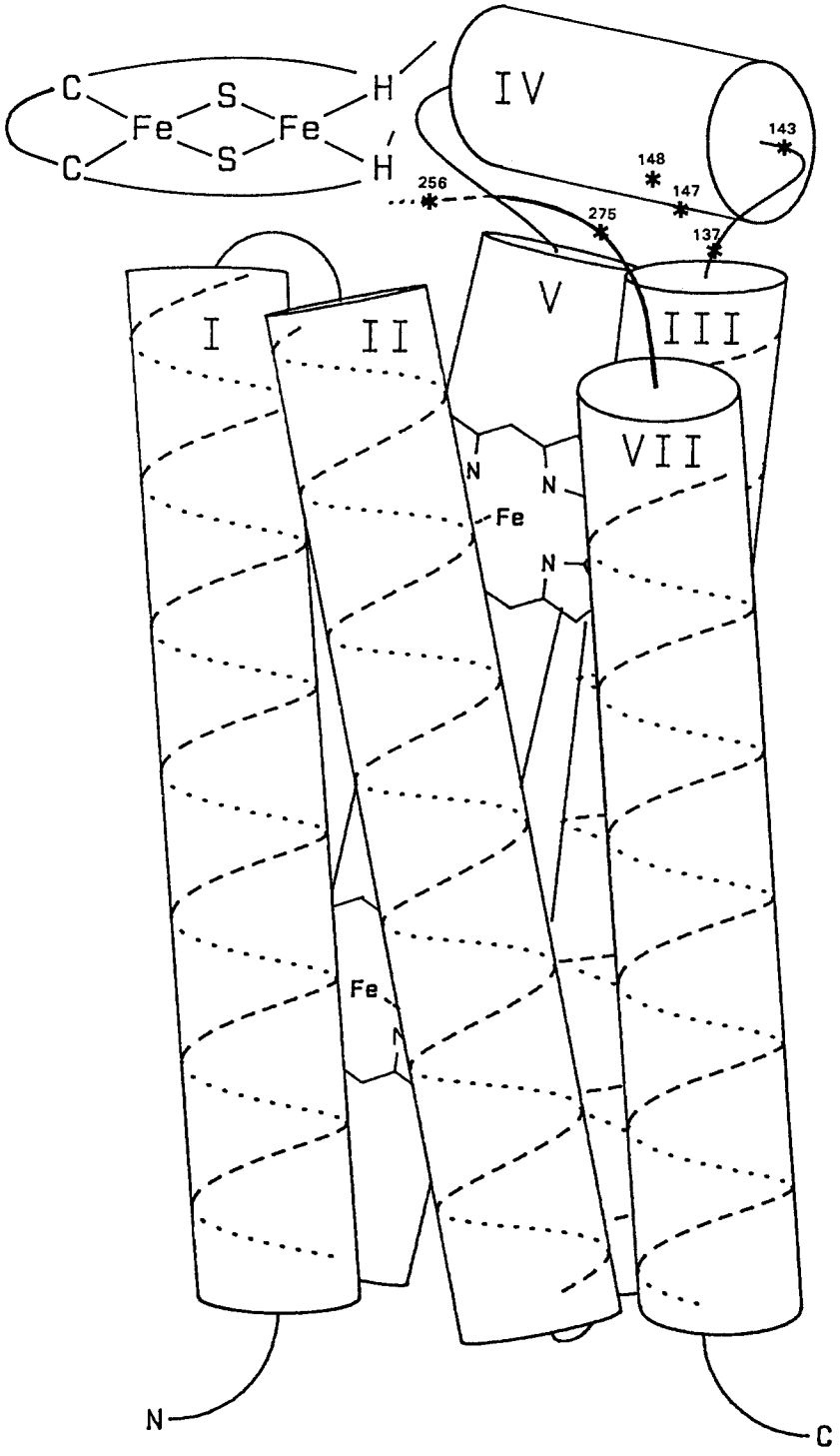


**Fig. 6.** 4-$\alpha$-Helical bundle of cytochrome *b* formed by the helices I, II, III, and V. The P-side of the membrane is on top. The two heme *b* centers are bound between helices II and V. Helix VII is shown next to helix III. Helix IV, the loop between helices VI and VII, and the iron–sulfur protein are on top of the helical bundle. The asterisks indicate the six residues where mutations alter the binding of inhibitors which are not in transmembrane helices.

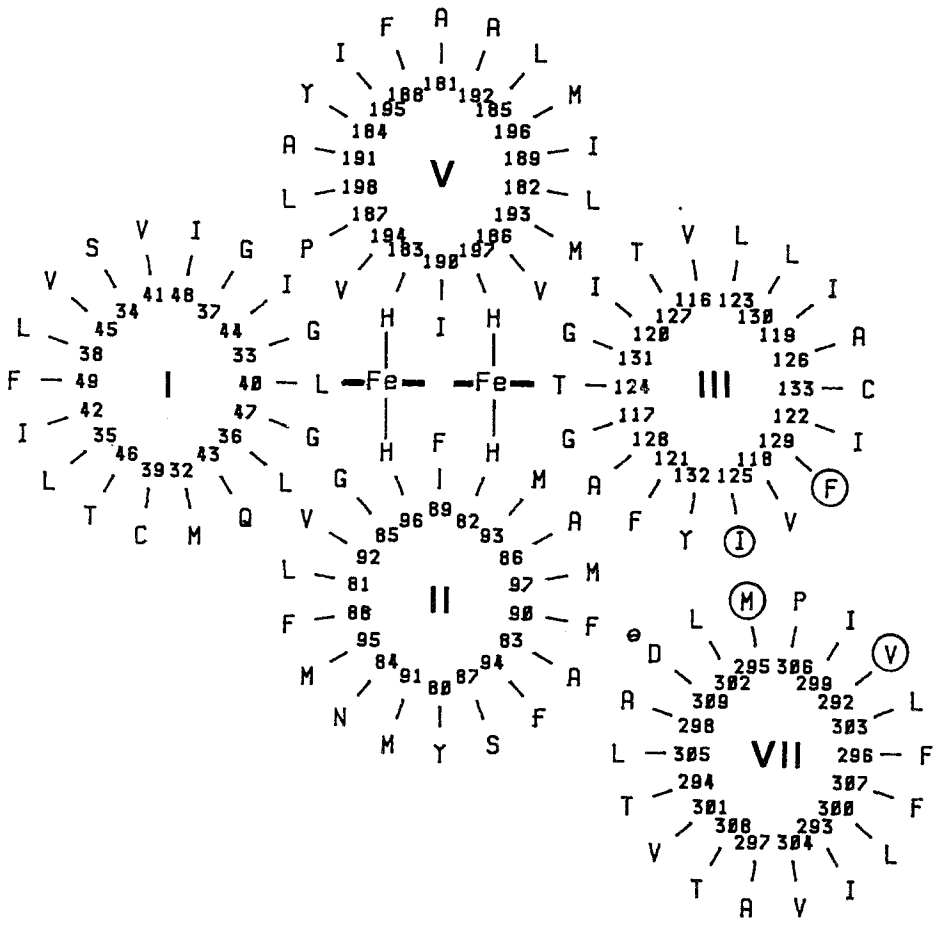


**Fig. 7.** Helical wheel representation of the 4-α-helical bundle of cytochrome *b* and helix VII. The view is from the P-side (top of Fig. 6). The residues in helices III and VII where mutations alter the binding of inhibitors are encircled.

building, and the analysis of the inhibitor data: The central core of cytochrome *b* constitutes an α-helical bundle (Link *et al.*, 1986). This bundle is formed by helices I to III and V (= helices A to D) of cytochrome *b* (Fig. 6). Helix VII (= helix F) is expected to be close to helix III if one assumes that mutations conferring resistance to the MOA inhibitors are within the same space (Fig. 7). Helix IV, the loop between helices VI and VII, and the cluster domain of the iron–sulfur protein are on top of the $Q_P$ pocket, shielding it from the aqueous environment.

When this structure is compared to the $Q_B$ site of the photoreaction center, the following differences are observed: The $Q_P$ pocket is formed by domains of two protein subunits. The $Q_P$ pocket seems to be considerably larger since it not only binds inhibitors which are large in size compared to photosynthetic inhibitors but may also accommodate two quinone molecules at a time (Ding *et al.*, 1992). Finally, at the $Q_P$ site, electrons are transferred to two different electron acceptors; it remains to be established whether this highly organized reaction involves different protein states ("catalytic switch"; Brandt *et al.*, 1991) or movement of quinone within the pocket.

## ACKNOWLEDGMENT

We thank B. Geier for stimulating discussion and for assistance in preparing Fig. 6, and A. Gießler for making information available prior to publication.

## REFERENCES

Becker, W. F., von Jagow, G., Anke, T., and Steglich, W. (1981). *FEBS Lett.* 132, 329–333.

Berden, J. A., and Slater, E. C. (1970). *Biochim. Biophys. Acta* **216**, 237–249.
Berden, J. A., and Slater, E. C. (1972). *Biochim. Biophys. Acta* **256**, 199–215.
Bowyer, J. R., Edwards, C. A., Ohnishi, T., and Trumpower, B. L. (1982). *J. Biol. Chem.* **257**, 8321–8330.
Brandt, U., and von Jagow, G. (1991a). *FEBS Lett.* **287**, 215–218.
Brandt, U., and von Jagow, G. (1991b). *Eur. J. Biochem.* **195**, 163–170.
Brandt, U., Schägger, H., and von Jagow, G. (1988). *Eur. J. Biochem.* **173**, 499–506.
Brandt, U., Haase, U., Schägger, H., and von Jagow, G. (1991). *J. Biol. Chem.* **266**, 19958–19964.
Daldal, F., Tokito, M. K., Davidson, E., and Faham, M. (1989). *EMBO J.* **8**, 3951–3961.
Ding, H., Robertson, D. E., Daldal, F., and Dutton, P. L. (1992). *Biochemistry* **31**, 3144–3158.
di Rago, J.-P., Copée, J.-Y., and Colson, A.-M. (1989). *J. Biol. Chem.* **264**, 14543–14548.
di Rago, J.-P., Netter, P., and Slonimski, P. P. (1990a). *J. Biol. Chem.* **265**, 3332–3339.
di Rago, J.-P., Netter, P., and Slonimski, P. P. (1990b). *J. Biol. Chem.* **265**, 15750–15757.
Geier, B. M., Schägger, H., Brandt, U., and von Jagow, G. (1992). *Eur. J. Biochem.* **208**, 375–380.
González-Halphen, D., Vazques-Acevedo, M., and Garcia-Ponce, B. (1991). *J. Biol. Chem.* **266**, 3870–3876.
Gu, L.-q., Yu, L., and Yu, C.-A. (1990). *Biochim. Biophys. Acta* **1015**, 482–492.
Howell, N. (1990). *Biochemistry* **29**, 8970–8977.
Howell, N., and Gilbert K. (1988). *J. Mol. Biol.* **203**, 607–618.
Link, T. A., Schägger, H., and von Jagow, G. (1986). *FEBS Lett.* **204**, 9–15.
Link, T. A., Hagen, W. R., Pierik, A. J., Assmann, C., and von Jagow, G. (1992). *Eur. J. Biochem.* **208**, 685–691.
Lorusso, M., Cocco, T., Sardanelli, A. M., Minuto, M., Bonomi, F., and Papa, S. (1991). *Eur. J. Biochem.* **197**, 555–561.
Matsuura, K., Bowyer, J. R., Ohnishi, T., and Dutton, P. L. (1983). *J. Biol. Chem.* **258**, 1571–1579.
Mitchell, P. (1976). *J. Theor. Biol.* **62**, 327–367.
Ohnishi, T., Brandt, U., and von Jagow, G. (1988). *Eur. J. Biochem.* **176**, 385–389.
Page, M. I., and Jencks, W. P. (1971). *Proc. Natl. Acad. Sci. USA* **68**, 1678–1683.
Prince, R. C., and Dutton, P. L. (1976). *FEBS Lett.* **65**, 117–119.
Rich, P. R., Jeal, A. E., Madgwick, S. A., and Moody, A. J. (1990). *Biochim. Biophys. Acta Bio-Energ.* **1018**, 29–40.
Robertson, D. E., Daldal, F., and Dutton, P. L. (1990). *Biochemistry* **29**, 11249–11260.
Saitoh, I., Miyoshi, H., Shimizu, R., and Iwamura, H. (1992). *Eur. J. Biochem.* **209**, 73–79.
Schägger, H., Hagen, Th., Roth, B., Brandt, U., Link, T.A., and von Jagow, G. (1990). *Eur. J. Biochem.* **190**, 123–130.
Schulz, G. E., and Schirmer, R. H. (1979). *Principles of Protein Structure*, Springer-Verlag, New York/Berlin/Heidelberg/Tokyo.
Sinning, I., Michel, H., Mathis, P., and Rutherford, A.W. (1989). *Biochemistry* **28**, 5544–5553.
Thierbach, G., and Reichenbach, H., (1981). *Biochim. Biophys. Acta* **638**, 282–289.
Thierbach, G., Kunze, B., Reichenbach, H., and Höfle, G. (1984). *Biochim. Biophys. Acta* **765**, 227–235.
Tron, T., and Lemesle-Meunier, D. (1990). *Curr. Genet.* **18**, 413–419.
Tron, T., Crimi, M., Colson, A.-M., and Degli Esposti, M. (1991). *Eur. J. Biochem.* **199**, 753–760.
Trumpower, B. L. (1981). *Biochim. Biophys. Acta* **639**, 129–155.
Trumpower, B. L. (1990). *J. Biol. Chem.* **265**, 11409–11412.
Trumpower, B. L., and Haggerty, J. G. (1980). *J. Bioenerg. Biomembr.* **12**, 151–164.
van Ark, G., and Berden, J. A. (1977). *Biochim. Biophys. Acta* **459**, 119–137.
von Jagow, G., and Brandt, U. (1991). *Electron and Proton Transfer in Chemistry and Biology* (Müller, A., and Junge, W., eds.), Elsevier, Amsterdam.
von Jagow, G., and Engel, W. D. (1981). *FEBS Lett.* **136**, 19–24.
von Jagow, G., and Link, T. A. (1986). *Methods Enzymol.* **126**, 253–271.
von Jagow, G., and Ohnishi, T. (1985). *FEBS Lett.* **185**, 311–315.
von Jagow, G., Ljungdahl, P. O., Graf, P., Ohnishi, T., and Trumpower, B. L. (1984). *J. Biol. Chem.* **259**, 6318–6326.
von Jagow, G., Link, T. A., and Ohnishi, T. (1986). *J. Bioenerg. Biomembr.* **18**, 157–179.